Controlled Growth of the Self-Modulation of a Relativistic Proton Bunch in Plasma

L. Verra[1,2,3,*] G. Zevi Della Porta,[1] J. Pucek,[2] T. Nechaeva,[2] S. Wyler,[4] M. Bergamaschi,[2] E. Senes,[1]
E. Guran,[1] J. T. Moody,[2] M. Á. Kedves,[5] E. Gschwendtner,[1] and P. Muggli[2]

(AWAKE Collaboration)

R. Agnello,[4] C. C. Ahdida,[1] M. C. A. Goncalves,[1] Y. Andrebe,[4] O. Apsimon,[6,7] R. Apsimon,[7,8] J. M. Arnesano,[1]
A.-M. Bachmann,[2] D. Barrientos,[1] F. Batsch,[2] V. Bencini,[1,9] P. Blanchard,[4] P. N. Burrows,[9] B. Buttenschön,[10] A. Caldwell,[2]
J. Chappell,[11] E. Chevallay,[1] M. Chung,[12] D. A. Cooke,[11] C. Davut,[7,13] G. Demeter,[5] A. C. Dexter,[7,8] S. Doebert,[1]
F. A. Elverson,[1] J. Farmer,[1,2] A. Fasoli,[4] V. Fedosseev,[1] R. Fonseca,[14,15] I. Furno,[4] A. Gorn,[16,17] E. Granados,[1]
M. Granetzny,[18] T. Graubner,[19] O. Grulke,[10,20] V. Hafych,[2] J. Henderson,[7,21] M. Hüther,[2] V. Khudiakov,[22,16]
S.-Y. Kim,[12,1] F. Kraus,[19] M. Krupa,[1] T. Lefevre,[1] L. Liang,[7,13] S. Liu,[23] N. Lopes,[15] K. Lotov,[16,17] M. Martinez Calderon,[1]
S. Mazzoni,[1] D. Medina Godoy,[1] K. Moon,[12] P. I. Morales Guzmán,[2] M. Moreira,[15] E. Nowak,[1] C. Pakuza,[9]
H. Panuganti,[1] A. Pardons,[1] K. Pepitone,[24] A. Perera,[7,6] A. Pukhov,[22] R. L. Ramjiawan,[1,9] S. Rey,[1] O. Schmitz,[18]
F. Silva,[25] L. Silva,[15] C. Stollberg,[4] A. Sublet,[1] C. Swain,[7,6] A. Topaloudis,[1] N. Torrado,[15] P. Tuev,[16,17] F. Velotti,[1]
V. Verzilov,[23] J. Vieira,[15] M. Weidl,[26] C. Welsch,[7,6] M. Wendt,[1] M. Wing,[11] J. Wolfenden,[7,6] B. Woolley,[1]
G. Xia,[7,13] V. Yarygova,[16,17] and M. Zepp[18]

[1]*CERN, 1211 Geneva 23, Switzerland*
[2]*Max Planck Institute for Physics, 80805 Munich, Germany*
[3]*Technical University Munich, 80805 Munich, Germany*
[4]*Ecole Polytechnique Federale de Lausanne (EPFL), Swiss Plasma Center (SPC),*
1015 Lausanne, Switzerland
[5]*Wigner Research Centre for Physics, 1121 Budapest, Hungary*
[6]*University of Liverpool, Liverpool L69 7ZE, United Kingdom*
[7]*Cockcroft Institute, Warrington WA4 4AD, United Kingdom*
[8]*Lancaster University, Lancaster LA1 4YB, United Kingdom*
[9]*John Adams Institute, Oxford University, Oxford OX1 3RH, United Kingdom*
[10]*Max Planck Institute for Plasma Physics, 17491 Greifswald, Germany*
[11]*UCL, London WC1 6BT, United Kingdom*
[12]*UNIST, Ulsan 44919, Republic of Korea*
[13]*University of Manchester, Manchester M13 9PL, United Kingdom*
[14]*ISCTE—Instituto Universitéario de Lisboa, 1049-001 Lisbon, Portugal*
[15]*GoLP/Instituto de Plasmas e Fusão Nuclear, Instituto Superior Técnico, Universidade de Lisboa,*
1049-001 Lisbon, Portugal
[16]*Budker Institute of Nuclear Physics SB RAS, 630090 Novosibirsk, Russia*
[17]*Novosibirsk State University, 630090 Novosibirsk , Russia*
[18]*University of Wisconsin, Madison, Wisconsin 53706, USA*
[19]*Philipps-Universität Marburg, 35032 Marburg, Germany*
[20]*Technical University of Denmark, 2800 Kgs. Lyngby, Denmark*
[21]*Accelerator Science and Technology Centre, ASTeC, STFC Daresbury Laboratory,*
Warrington WA4 4AD, United Kingdom
[22]*Heinrich-Heine-Universität Düsseldorf, 40225 Düsseldorf, Germany*
[23]*TRIUMF, Vancouver, Canada*
[24]*Angstrom Laboratory, Department of Physics and Astronomy, 752 37 Uppsala, Sweden*
[25]*INESC-ID, Instituto Superior Técnico, Universidade de Lisboa, 1049-001 Lisbon, Portugal*
[26]*Max Planck Institute for Plasma Physics, 80805 Munich, Germany*

A long, narrow, relativistic charged particle bunch propagating in plasma is subject to the self-modulation (SM) instability. We show that SM of a proton bunch can be seeded by the wakefields driven by a preceding electron bunch. SM timing reproducibility and control are at the level of a small fraction of the modulation period. With this seeding method, we independently control the amplitude of the seed wakefields with the charge of the electron bunch and the growth rate of SM with the charge of the proton bunch. Seeding leads to larger growth of the wakefields than in the instability case.

Introduction.—Instabilities are of paramount importance in plasma physics [1]. Similar instabilities occur in vastly different plasmas—from astrophysical [2,3] to laboratory [4] and fusion [5] to quantum [6] and even to quark-gluon plasmas [7]. They can be disruptive and must then be suppressed, or beneficial and must then be controlled. Charged particle beams propagating in plasma are subject to a number of instabilities, including different occurrences of the two-stream instability [8,9]. In the case of a long, narrow, relativistic charged particle bunch, the instability is transverse and it is called the self-modulation instability (SMI) [10].

Relativistic charged particle bunches traveling in plasma leave behind a perturbation in the plasma electron density. This perturbation provides a restoring force that induces an oscillation of plasma electrons with angular frequency $\omega_{pe} = \sqrt{n_{pe}e^2/m_e\varepsilon_0}$, where n_{pe} is the plasma electron density, e and m_e are the electron charge and mass, ε_0 is the vacuum permittivity. The local charge non-neutrality sustains fields with transverse and longitudinal components, known as wakefields, that can have amplitudes appealing for high-gradient particle acceleration [11,12].

SMI [10] develops when the bunch duration is much longer than the period of the wakefields: $\sigma_t \gg T_{pe} = 2\pi/\omega_{pe}$. Transverse wakefields act back on the bunch, modulating its radius and thus its charge density. The modulated distribution drives enhanced wakefields, causing the growth of SMI that, at saturation, leaves the long bunch fully modulated into a train of microbunches with periodicity $\sim T_{pe}$. The timing of the microbunches along the train is tied to that of the wakefields since microbunches develop in their focusing phase.

When a long proton (p^+) bunch enters a preionized plasma, SMI develops from wakefields driven by noise [13] or by imperfections in the incoming bunch charge distribution [14]. Thus, the initial conditions vary from event to event and so do the timing and amplitude of the wakefields. However, the outcome can be controlled by seeding the instability, i.e., by fixing the initial conditions from which the instability grows.

Seeding requires driving initial transverse wakefields with amplitude larger than those driven by the noise or imperfections in the bunch so that the self-modulation (SM) develops from a well-defined time, and with well-defined initial amplitude and growth rate. We demonstrated

experimentally that a high-energy, long p^+ bunch undergoes SMI when traveling in plasma [15], and that the resulting microbunch train resonantly excites large amplitude wakefields [16,17]. A relativistic ionization front (RIF) generating the plasma and copropagating within the p^+ bunch can provide the seed by the rapid onset of the beam-plasma interaction [14]. In this case, the amplitude of the seed wakefields and the growth rate of SM depend on the p^+ bunch density at the RIF and cannot be varied independently. Moreover, the front of the bunch propagates as if in vacuum and thus remains unmodulated.

The initial transverse seed wakefields can also be provided by a preceding charged particle bunch [18,19]. In this case, seeding amplitude and growth rate of SM can be varied independently. Moreover, as the seed wakefields act on the whole p^+ bunch, the entire bunch self-modulates. This removes the risk that the front of the bunch, left unmodulated by RIF seeding, self-modulates in a second plasma required for a high-energy accelerator [20,21].

The protons that are defocused out of the wakefields are probes for the amplitude of the wakefields at early distances along plasma, during SM growth, before saturation [16,22]. Theoretical and numerical simulation results [10,23–25] show that, in the linear regime, the amplitude of the transverse wakefields along the bunch (t) and along the plasma (z) grows as $W_\perp(t, z) = W_{\perp 0} \exp{(\Gamma(t, z)z)}$. In the case of seeding with an electron (e^-) bunch, the amplitude of the initial wakefields $W_{\perp 0}(z = 0)$ depends solely on the e^- bunch parameters, while the growth rate of SM $\Gamma(t, z)$ depends solely on those of the p^+ bunch. The radial extent reached by defocused protons a distance downstream of the plasma is proportional to the transverse momentum they acquire from these wakefields, and therefore increases with the growth of SM.

In this Letter, we demonstrate with experimental results that SM of a long, relativistic p^+ in plasma can be seeded by a preceding e^- bunch. We show that the growth of SM increases when increasing the charge of the seed e^- bunch Q_e or the charge of the p^+ bunch Q_p. We attribute these changes to a change in the amplitude of the transverse seed wakefields $W_{\perp 0}(Q_e)$ or in the SM growth rate $\Gamma(Q_p)$. These observations are possible because the e^- bunch effectively seeds SM and they are in agreement with theoretical and simulation predictions [10,23,25,26]. When seeding, the growth of the process is larger than
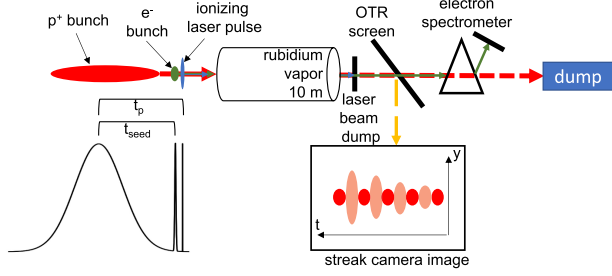
FIG. 1. Schematic of the experimental setup: the ionizing laser pulse enters the vapor source t_p ahead of the p^+ bunch center and ionizes the rubidium atoms, creating the plasma. The seed e^- bunch follows, t_{seed} ahead of the p^+ bunch. The optical transition radiation produced at a screen positioned 3.5 m downstream of the plasma exit is imaged on the entrance slit of a streak camera. A schematic example of a time-resolved image of the self-modulated p^+ bunch provided by the streak camera is shown in the inset. The magnetic spectrometer is located downstream of the screen.

in the SMI case [10]. We also observe adiabatic focusing of the front of the p^+ bunch, where the growth of SM is small. In addition, e^- bunch seeding allows for the timing of the process to be controlled at the submodulation-period, picosecond timescale.

Experimental Setup.—The measurements took place in the context of the AWAKE experiment [27], whose goal is to accelerate e^- bunches to GeV energies, ultimately for high-energy physics applications [28].

Figure 1 shows a schematic of the experimental setup. A 10-m-long source provides rubidium vapor density adjustable in the $n_{vap} = (0.5$–$10) \times 10^{14}$ cm^{-3} range [27].

The density is measured to better than 0.5% [29] at the source ends. An $\sim$120 fs, $\sim$100 mJ laser pulse ($\lambda = 780$ nm) produces a RIF that creates the plasma by ionizing the vapor (RbI $\rightarrow$ RbII). Previous experiments [15] showed that the RIF ionizes $\sim$100% of the vapor along its path, producing an $\sim$2-mm-diameter plasma column with density equal to that of the vapor. The RIF is placed $t_p = 620$ ps ($\sim$2.6σ_t) ahead of the center of the 400 GeV/c, $\sigma_t \sim 240$ ps, p^+ bunch provided by the CERN SPS. Therefore, it does not seed SM [14]. The p^+ bunch is synchronized with the RIF with root mean square (rms) variation of 15 ps $\ll \sigma_t$, which is therefore negligible.

Optical transition radiation (OTR) is emitted when protons enter an aluminum-coated silicon wafer, positioned 3.5 m downstream of the plasma exit. The OTR is imaged onto the entrance slit of a streak camera that provides time-resolved images of the charge density distribution of the p^+ bunch (t, y) [30] in a $\sim$180-μm-wide slice (the spatial resolution of the optical system) near the propagation axis. The streak camera temporal resolution is $\sim$2 ps in the 210 ps time window (Fig. 2), sufficient to resolve the microbunch train as the plasma periods are $T_{pe} = 11.04$ and 11.38 ps, for the values of n_{pe} used in this experiment. It can also produce ns timescale images with lower time resolution (Fig. 3). An ultraviolet pulse derived from the same laser oscillator as that producing the RIF generates an 18.3 MeV e^- bunch in a photoinjector and booster cavity [31]. The e^- bunch and the RIF have a relative rms timing jitter < 1 ps ($\ll T_{pe}$) [32]. The delay t_{seed} between the e^- and the p^+ bunch centers can be adjusted using a delay stage. We use a magnetic spectrometer [33] to measure the
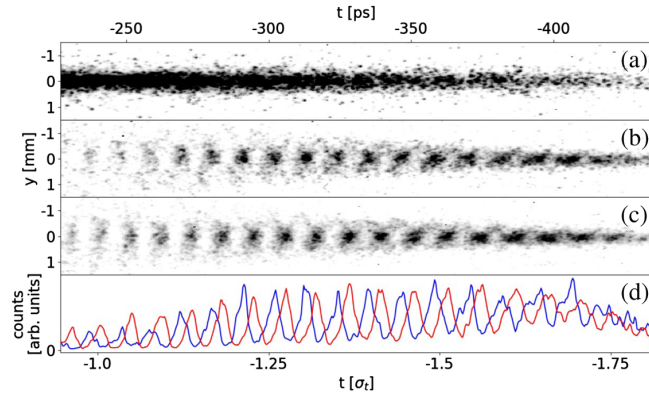

FIG. 2. Time-resolved images (t, y) of the p^+ bunch at the OTR screen obtained by averaging 10 single-event images (210 ps, $Q_p = 14.7$ nC). Bunch center at $t = 0$ ps, the bunch travels from left to right. Horizontal axis: time along the bunch normalized to the incoming bunch duration σ_t. (a) No plasma (incoming bunch). (b) Plasma ($n_{pe} = 1.02 \times 10^{14}$ cm^{-3}) and e^- bunch with $Q_e = 249$ pC, $t_{seed} = 614$ ps ahead of the p^+ bunch center. (c) Same as (b) but e^- bunch delayed by 6.7 ps ($t_{seed} = 607.3$ ps). All images have the same color scale. (d) On-axis time profiles of (b) (blue line) and (c) (red line) obtained by summing counts over $-0.217 \leq y \leq 0.217$ mm.
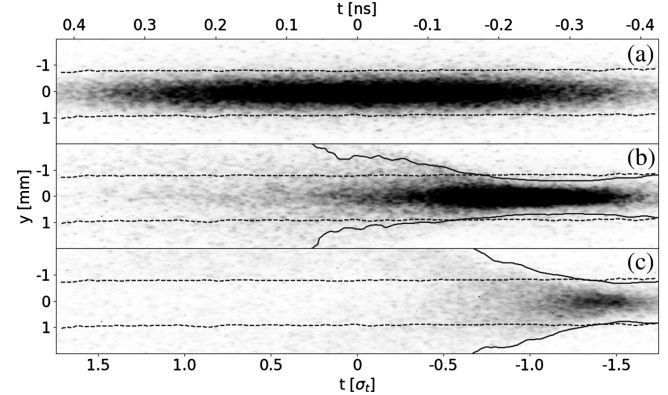
FIG. 3. Time-resolved images (t, y) of the p^+ bunch (1.1 ns, $Q_p = 14.7$ nC) obtained by averaging 10 single-event images. (a) No plasma (incoming bunch). (b) Plasma ($n_{pe} = 0.97 \times 10^{14}$ cm^{-3}) and no e^- bunch (SMI). (c) Plasma and e^- bunch with $Q_e = 249$ pC (seeded SM). All images have the same color scale. Black dashed lines in (a) and continuous lines in (b) and (c) indicate, for each time column of the images, the points where the transverse distribution reaches 20% of its peak value. The distance between the lines is the transverse extent w_{off} (a) and w (b), (c). Dashed lines of (a) also plotted in (b) and (c) for reference.

energy spectrum of the e^- bunch after propagation with and without plasma [34].

We use a bleed-through of the ionizing laser pulse, thus also synchronized with the e^- bunch at the sub-ps timescale [35], to determine on the time-resolved images the bunch train timing with respect to that of the e^- bunch. This is necessary to circumvent the ~5 ps rms jitter ($\sim T_{pe}/2$) of the triggering system.

Experimental Results.—We first present a new and important result that is necessary for the measurements presented hereafter: the seeding of SM by the e^- bunch. The incoming p^+ bunch with $Q_p = (14.7 \pm 0.2)$ nC has a continuous charge distribution (Fig. 2(a), no plasma) with an approximately 2D-Gaussian (t, y) charge density profile. With the plasma ($n_{pe} = 1.02 \times 10^{14}$ cm^{-3}) and the $Q_e = (249 \pm 17)$ pC e^- bunch placed $t_{\text{seed}} = 612$ ps ahead of the center of the p^+ bunch, we observe the clear formation of a train of microbunches on the image resulting from the average of ten consecutive single-event images [Fig. 2(b)]. This indicates that SM is reproducible from event to event. The period of the modulation is 11.3 ps, close to T_{pe}, as expected from SM [10,15]. We measure the timing variation of the microbunch train with respect to the e^- bunch by performing a discrete Fourier transform (see the Supplemental Material of [14]) analysis of the on-axis time profile of single-event images. The rms timing variation is $\Delta t_{\text{rms}} = 0.06 T_{pe}$, demonstrating that the e^- bunch effectively seeds SM. The same measurement without the e^- bunch yields $\Delta t_{\text{rms}} = 0.26 T_{pe}$, consistent with uniform variation of the timing over T_{pe} ($\Delta t_{\text{rms}} = 0.29 T_{pe}$), confirming the occurrence of SMI, as was also observed in [14].

We also observe seeding of SM with $Q_p = (46.9 \pm 0.5)$ nC and the same value of $Q_e = 249$ pC, i.e., with p^+ bunch and plasma parameters similar to those of [14]. This indicates that the e^- bunch drives transverse wakefields with amplitude exceeding the seeding threshold value of (2.8–4.0) MV/m, determined in [14] when seeding with RIF. The amplitude thus also exceeds that for the lower $Q_p = 14.7$ nC (Fig. 2) since the seeding threshold is expected to scale with Q_p.

Figure 2(c) shows an averaged time-resolved image obtained after delaying the seed e^- bunch timing by 6.7 ps with respect to the case of Fig. 2(b). The bunch train is again clearly visible and timing analysis shows an rms variation of $0.07 T_{pe}$, confirming again the seeding of SM. Figure 2(d) shows that the temporal profile of Fig. 2(c) (red curve) is shifted in time by (7.2 ± 1.0) ps with respect to that of Fig. 2(b) (blue curve). This demonstrates that the timing of the p^+ bunch modulation and thus also the timing of the wakefields are tied to that of the seed within a small fraction of T_{pe}.

As the amplitude of the wakefields grows along the bunch and along the plasma [15,16], one may expect them to produce a smaller size of the successive microbunches at the plasma exit, possibly also with larger emittance due to the nonlinear nature of the transverse wakefields. These two effects are the likely causes for the increase in transverse size of the microbunches along the train observed in Figs. 2(b) and 2(c), as the OTR screen is positioned 3.5 m downstream of the plasma exit. We also note that the p^+ bunch self-modulates starting from the visible front of the bunch [$t > -1.82\sigma_t$ on Figs. 2(b) and 2(c)], as the seed wakefields act on the entire bunch, and that on these figures the charge density at the bunch front is higher than in the case without plasma [Fig. 2(a)]. This is due to the focusing effect associated with the formation of the microbunches and to global plasma adiabatic focusing (see Fig. 3).

We measure the transverse extent of the p^+ bunch distribution along the bunch on 1.1 ns, time-resolved images (Fig. 3). We define this extent w for each time column of the image as the distance between the two points ($\pm y$) where the transverse distribution reaches 20% of its peak value, when detectable. In the case without plasma (Fig. 3(a), incoming bunch), $w_{\text{off}} = 1.7$ mm is constant along the bunch (black dashed line) and corresponds to the $\sigma_y \sim 0.37$ mm rms size of the Gaussian bunch at the screen.

In the case with plasma (hereafter $n_{pe} = 0.97 \times 10^{14}$ cm^{-3}) and no e^- bunch [SMI [14], Fig. 3(b)], the transverse extent (black continuous lines) indicates that the effect of plasma adiabatic focusing dominates first, i.e., w decreases, due to the cancellation of the p^+ bunch space-charge field by the plasma electrons ($t < -0.8\sigma_t$). Then the effect of defocusing due to SM development dominates and w increases.

We note that the time resolution of these images is not sufficient to evidence the microbunch structure and the charge distribution appears continuous along the bunch.

In the case with plasma and e^- bunch ($Q_e = 249$ pC, seeded SM, Fig. 3(c), all other parameters kept constant), the same focusing effect as in the SMI case first dominates, but the effect of defocusing starts earlier: $t \sim -1.5\sigma_t$ rather than $t \sim -0.8\sigma_t$ [Fig. 3(b)].

Figure 4(a) shows that, when increasing the charge of the seed bunch Q_e, the width w along the bunch initially decreases, following the same curve in all cases, due to the effect of adiabatic focusing. It then increases with SM growth, reaching the value of the case without plasma (w_{off}) earlier along the bunch, for larger Q_e (red points). Since the global focusing effect is equal in all cases ($Q_p = $ const), this shows that an increase in Q_e causes SM defocusing effect to dominate earlier along the bunch. Beyond this time, w increases monotonically. With increasing Q_e, w reaches larger values at any given time, as shown in Fig. 4(b) for two times along the bunch (blue points: $t = -1.19\sigma_t$, red points: $t = -0.84\sigma_t$; first and last t when $w > w_{\text{off}}$ for $Q_e > 0$ and all measurements provide a value).

Measurement of the energy spectrum of the seed e^- bunch (not shown) [34], and numerical simulation results [36] indicate that the amplitude of the wakefields driven by
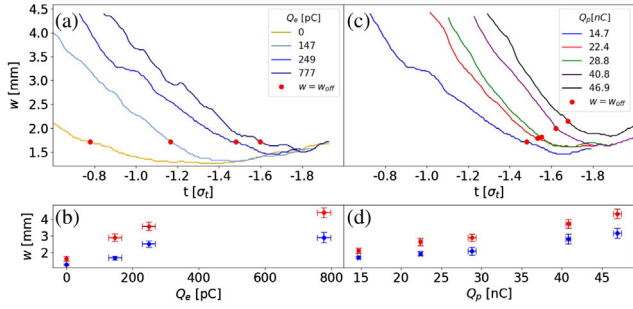
FIG. 4. Top row: transverse extent w along the p^+ bunch as a function of time along the bunch normalized to the incoming bunch duration σ_t. (a) Varying the e^- bunch charge (see legend), $Q_e = 0$ (SMI), $Q_e > 0$ (seeded SM), $Q_p = 14.7$ nC. (c) Varying the p^+ bunch charge Q_p (see legend), $Q_e = 249$ pC. Red points indicate the time along the bunch when $w = w_{\text{off}}$. Bottom row: (b) w as a function of Q_e at $t = -1.19$ (blue points) and $t = -0.84\sigma_t$ (red points). (d) w as a function of Q_p at $t = -1.48$ (blue points) and $t = -1.30\sigma_t$ (red points). The error bars indicate the standard deviation of w, and of Q_e and Q_p. Note: blue line: same data on (a) and (c).

the e^- bunch $W_{\perp 0}$ over the first ~ 2 m of plasma increases as a function of Q_e and exceeds 4 MV/m in all cases. The earlier occurrence of SM defocusing and the increase in w at all times when $w \geq w_{\text{off}}$ for larger Q_e are thus directly caused by the increase in amplitude of the seed wakefields $W_{\perp 0}(Q_e)$, since all other parameters were kept constant ($\Gamma(Q_p) = \text{const}$). Figure 4(a) also shows that in the SMI regime ($Q_e = 0$) the defocusing effect of SM dominates much later along the bunch ($\sim -0.78\sigma_t$) and w is much smaller than in the seeded regime ($Q_e > 0$). This lower growth can be attributed to the lower amplitude of the (uncontrolled) initial wakefields, as well as to a later start of SM along the bunch [14].

When increasing the p^+ bunch charge Q_p [Fig. 4(c)], we observe again that w increases at all times along the bunch when SM defocusing effect dominates, as also shown in Fig. 4(d) for two times along the bunch (blue points: $t = -1.48\sigma_t$, red points: $t = -1.30\sigma_t$; t chosen as in the previous case).

Measurements of $\sigma_{x,y}$ show that over the $Q_p = (14.7\text{–}46.9)$ nC range, $n_p \propto Q_p/\sigma_{x,y}^2$ changes only from 6.9 to 8.9×10^{12} cm^{-3} [37]. This is due to the fact that, when increasing Q_p, SPS produces a bunch with larger geometric emittance ϵ_g and thus larger transverse size $\sigma_{x,y} \propto \epsilon_g^{1/2}$. Figure 4(c) shows an increase of both adiabatic and SM growth effects with Q_p, as expected. The effect of SM defocusing dominates from an earlier time along the bunch, indicating that the effect of the increase in Q_p is stronger on SM than on adiabatic focusing. The SM growth rate has a weak dependency on Q_p ($\Gamma \propto n_p^{1/3} \propto (Q_p/\sigma_{x,y}^2)^{1/3}$ [10,23,25]); see above. However, the effect on w we observe on Fig. 4(c) is significant because measured after

exponentiation of SM. Also, Γ does not depend on the bunch emittance, which increases with Q_p and is known to decrease the growth of SM [38,39]. Therefore, the effect of Q_p on SM (all other parameters kept constant) is larger than observed on Fig. 4(c).

We note here that the measurement of w is not a direct measurement of the amplitude of the seed wakefields $W_{\perp 0}$ or growth rate Γ. However, changes in w are direct consequences of changes in $W_{\perp 0}(Q_e)$ and $\Gamma(Q_p)$. For a direct measurement of Γ all protons would have to leave the wakefields at the same position along the plasma and propagate ballistically an equal distance to the OTR screen. Numerical simulation results show that with the plasma of these experiments longer than the saturation length of SM [22], protons may leave the wakefields earlier or later depending on the amplitude of the wakefields and on the distance they are subject to them. However, simulation results also show monotonic increase of w, as observed in the experiments, and that w increases with increasing amplitude of the wakefields along the bunch.

Summary.—We demonstrated in experiments that a short e^- bunch can seed SM of a long p^+ bunch in plasma. We showed that when increasing the e^- (Q_e) or the p^+ (Q_p) bunch charge, the transverse extent of the p^+ bunch distribution w along the bunch (measured after the plasma) also increases. We attribute these changes to the change in amplitude of the seed wakefields ($Q_e \to W_{\perp 0}$) and in growth rate of SM ($Q_p \to \Gamma$), in agreement with theoretical and simulation results.

These results show that SM is well understood and can be well controlled. Control is key for optimization of the SM wakefields for particle acceleration [20,40].

*Corresponding author.
livio.verra@cern.ch

[1] B. Lehnert, Experimental evidence of plasma instabilities, Plasma Phys. 9, 301 (1967).

[2] A. M. Bykov, A. Brandenburg, M. A. Malkov, and S. M. Osipov, Microphysics of cosmic ray driven plasma instabilities, Space Sci. Rev. 178, 201 (2013).

[3] F. Haas, Neutrino oscillations and instabilities in degenerate relativistic astrophysical plasmas, Phys. Rev. E 99, 063209 (2019).

[4] F. F. Cap, Handbook on Plasma Instabilities, edited by F. F. Cap (Academic Press, New York, 1976).

[5] D. S. Montgomery, Two decades of progress in understanding and control of laser plasma instabilities in indirect drive inertial fusion, Phys. Plasmas 23, 055601 (2016).

[6] K. Sharma and U. Deka, Comprehensive review on various instabilities in semiconductor quantum plasma, Braz. J. Phys. 51, 1944 (2021).

[7] P. Arnold, J. Lenaghan, G. D. Moore, and L. G. Yaffe, Apparent Thermalization due to Plasma Instabilities in the Quark-Gluon Plasma, Phys. Rev. Lett. 94, 072302 (2005).

[8] D. T. Farley, Two-Stream Plasma Instability as a Source of Irregularities in the Ionosphere, Phys. Rev. Lett. 10, 279 (1963).

[9] O. Buneman, Excitation of Field Aligned Sound Waves by Electron Streams, Phys. Rev. Lett. 10, 285 (1963).

[10] N. Kumar, A. Pukhov, and K. Lotov, Self-Modulation Instability of a Long Proton Bunch in Plasmas, Phys. Rev. Lett. 104, 255003 (2010).

[11] T. Tajima and J. M. Dawson, Laser Electron Accelerator, Phys. Rev. Lett. 43, 267 (1979).

[12] P. Chen, J. M. Dawson, R. W. Huff, and T. Katsouleas, Acceleration of Electrons by the Interaction of a Bunched Electron Beam with a Plasma, Phys. Rev. Lett. 54, 693 (1985).

[13] K. V. Lotov, G. Z. Lotova, V. I. Lotov, A. Upadhyay, T. Tückmantel, A. Pukhov, and A. Caldwell, Natural noise and external wakefield seeding in a proton-driven plasma accelerator, Phys. Rev. ST Accel. Beams 16, 041301 (2013).

[14] F. Batsch, P. Muggli et al. (AWAKE Collaboration), Transition Between Instability and Seeded Self-Modulation of a Relativistic Particle Bunch in Plasma, Phys. Rev. Lett. 126, 164802 (2021).

[15] AWAKE Collaboration, Experimental Observation of Proton Bunch Modulation in a Plasma at Varying Plasma Densities, Phys. Rev. Lett. 122, 054802 (2019).

[16] M. Turner et al. (AWAKE Collaboration), Experimental Observation of Plasma Wakefield Growth Driven by the Seeded Self-Modulation of a Proton Bunch, Phys. Rev. Lett. 122, 054801 (2019).

[17] AWAKE Collaboration, Acceleration of electrons in the plasma wakefield of a proton bunch, Nature (London) 561, 363 (2018).

[18] M. Hüther and P. Muggli, Seeding of the self-modulation in a long proton bunch by charge cancellation with a short electron bunch, Nucl. Instrum. Methods Phys. Res., Sect. A 909, 67 (2018), 3rd European Advanced Accelerator Concepts workshop (EAAC2017).

[19] P. Muggli, P. I. Morales Guzman, A.-M. Bachmann, M. Hüther, M. Moreira, M. Turner, and J. Vieira, Seeding self-modulation of a long proton bunch with a short electron bunch, J. Phys. Condens. Matter 1596, 012066 (2020).

[20] P. Muggli, Physics to plan AWAKE run 2, J. Phys. Condens. Matter 1596, 012008 (2020).

[21] E. Gschwendtner, Awake Run 2 at CERN, Proceedings of the IPAC'21, International Particle Accelerator Conference, TUPAB159 (2021), 10.18429/JACoW-IPAC2021-TU-PAB159.

[22] M. Turner, P. Muggli et al. (AWAKE Collaboration), Experimental study of wakefields driven by a self-modulating proton bunch in plasma, Phys. Rev. Accel. Beams 23, 081302 (2020).

[23] A. Pukhov, N. Kumar, T. Tückmantel, A. Upadhyay, K. Lotov, P. Muggli, V. Khudik, C. Siemon, and G. Shvets, Phase Velocity and Particle Injection in a Self-Modulated Proton-Driven Plasma Wakefield Accelerator, Phys. Rev. Lett. 107, 145003 (2011).

[24] K. V. Lotov, Physics of beam self-modulation in plasma wakefield accelerators, Phys. Plasmas 22, 103110 (2015).

[25] C. B. Schroeder, C. Benedetti, E. Esarey, F. J. Grüner, and W. P. Leemans, Growth and Phase Velocity of Self-Modulated Beam-Driven Plasma Waves, Phys. Rev. Lett. 107, 145002 (2011).

[26] K. V. Lotov and P. V. Tuev, Plasma wakefield acceleration beyond the dephasing limit with 400 GeV proton driver, Plasma Phys. Controlled Fusion 63, 125027 (2021).

[27] P. Muggli et al. (AWAKE Collaboration), AWAKE readiness for the study of the seeded self-modulation of a 400 GeV proton bunch, Plasma Phys. Controlled Fusion 60, 014046 (2018).

[28] A. Caldwell and M. Wing, VHEeP: A very high energy electron-proton collider, Eur. Phys. J. C 76, 463 (2016).

[29] F. Batsch, M. Martyanov, E. Oez, J. Moody, E. Gschwendtner, A. Caldwell, and P. Muggli, Interferometer-based high-accuracy white light measurement of neutral rubidium density and gradient at AWAKE, Nucl. Instrum. Methods Phys. Res., Sect. A 909, 359 (2018), 3rd European Advanced Accelerator Concepts workshop (EAAC2017).

[30] K. Rieger, A. Caldwell, O. Reimann, R. Tarkeshian, and P. Muggli, GHz modulation detection using a streak camera: Suitability of streak cameras in the AWAKE experiment, Rev. Sci. Instrum. 88, 025110 (2017).

[31] K. Pepitone, S. Doebert, G. Burt, E. Chevallay, N. Chritin, C. Delory, V. Fedosseev, C. Hessler, G. McMonagle, O. Mete, V. Verzilov, and R. Apsimon, The electron accelerator for the AWAKE experiment at CERN, Nucl. Instrum. Methods Phys. Res., Sect. A 829, 73 (2016), 2nd European Advanced Accelerator Concepts Workshop—EAAC 2015.

[32] A.-M. Bachmann, Self-modulation development of a proton bunch in plasma, Ph.D thesis, Technical University Munich Report No. CERN-THESIS-2021-094, 2021.

[33] J. Bauche et al., A magnetic spectrometer to measure electron bunches accelerated at AWAKE, Nucl. Instrum. Methods Phys. Res., Sect. A 940, 103 (2019).

[34] L. Verra, G. Zevi Della Porta, K.-J. Moon, A.-M. Bachmann, E. Gschwendtner, and P. Muggli, 47th EPS Conference on Plasma Physics (2021), http://ocs.ciemat.es/EPS2021PAP/pdf/P3.2011.pdf.

[35] F. Batsch, Setup and characteristics of a timing reference signal with sub-ps accuracy for AWAKE, J. Phys.: Conf. Ser. **1596,** 012006 (2020).

[36] K.-J. Moon *et al.* (to be published).

[37] When Q_p varies in the range (14.8–47.2) nC, the transverse size at the plasma entrance and normalized emittance of the p^+ bunch vary accordingly in the ranges $\sigma_{x,y} = (0.11, 0.10\text{–}0.18, 0.17)$ mm and $\epsilon_N = \beta_z \gamma \epsilon_g = (1.4\text{–}2.9)$ mm mrad (β_z is the ratio of the velocity to c, γ is the Lorentz factor), respectively, and the bunch duration remains in the range $\sigma_t \sim (236\text{–}255)$ ps, leading to the bunch density values quoted in the text.

[38] A. Gorn, M. Turner *et al.* (AWAKE Collaboration), Proton beam defocusing in AWAKE: Comparison of simulations and measurements, Plasma Phys. Controlled Fusion **62,** 125023 (2020).

[39] K. V. Lotov, Effect of beam emittance on self-modulation of long beams in plasma wakefield accelerators, Phys. Plasmas **22,** 123107 (2015).

[40] Veronica K. Berglyd Olsen, E. Adli, and P. Muggli, Emittance preservation of an electron beam in a loaded quasilinear plasma wakefield, Phys. Rev. Accel. Beams **21,** 011301 (2018).